Published in final edited form as:
Cancer Res. 2009 August 15; 69(16): 6747–6755. doi:10.1158/0008-5472.CAN-08-3949.

Osteoclast derived matrix metalloproteinase-7 but not matrix metalloproteinase-9 contributes to tumor induced osteolysis

Sophie Thiolloy[1], **Jennifer Halpern**[2], **Ginger E. Holt**[2], **Herbert S. Schwartz**[2], **Gregory R. Mundy**[3], **Lynn M. Matrisian**[2], and **Conor C. Lynch**[*,1,2]

Sophie Thiolloy: sophie.thiolloy@vanderbilt.edu; Jennifer Halpern: jennifer.halpern@vanderbilt.edu; Ginger E. Holt: ginger.e.holt@vanderbilt.edu; Herbert S. Schwartz: herbert.s.schwartz@vanderbilt.edu; Gregory R. Mundy: gregory.r.mundy@vanderbilt.edu; Lynn M. Matrisian: lynn.matrisian@vanderbilt.edu; Conor C. Lynch: conor.lynch@vanderbilt.edu

[1]Department of Cancer Biology, Vanderbilt University, Nashville, TN. 37232. USA

[2]Department of Orthopaedics and Rehabilitation, Vanderbilt University, Nashville, TN. 37232. USA

[3]Department of Vanderbilt Center for Bone Biology, Vanderbilt University, Nashville, TN. 37232. USA

Abstract

The matrix metalloproteinases, MMP-2, -3, -7, -9 and -13 are highly expressed in the tumor-bone microenvironment and of these, MMP-7 and MMP-9 were found to be localized to bone resorbing osteoclasts in human breast to bone metastases. In a bid to define the roles of host derived MMP-7 and MMP-9 in the tumor-bone microenvironment, the tibia of MMP-7 and MMP-9 null mice were injected with osteolytic luciferase tagged mammary tumor cell lines. Our data demonstrates that osteoclast derived MMP-7 significantly contributes to tumor growth and tumor induced osteolysis while osteoclast derived MMP-9 had no impact on these processes. MMP-7 is capable of processing a number of non-matrix molecules to soluble active forms that have profound effects on cell-cell communication such as RANKL, a crucial mediator of osteoclast precursor recruitment and maturation. Therefore, the ability of osteoclast derived MMP-7 to promote RANKL solubilization in the tumor-bone microenvironment was explored. Results revealed that levels of soluble RANKL were significantly lower in the MMP-7 null mice compared to wild type controls. In keeping with this observation, MMP-7 null mice had significantly fewer osteoclast numbers at the tumor-bone interface compared to the wild-type controls. In summary, we propose that the solubilization of RANKL by MMP-7 is a potential mechanism through which MMP-7 mediates mammary tumor induced osteolysis. Our studies indicate that the selective inhibition of MMP-7 in the tumor-bone microenvironment may be of benefit for the treatment of lytic breast to bone metastases.

Keywords

breast to bone metastasis; osteoclasts; osteolysis; matrix metalloproteinase; MMP-7; MMP-9; receptor activator of nuclear kappa B ligand; RANKL

Introduction

Bone metastasis is a common event during breast cancer progression with the resultant lesions often being osteolytic (1). In the bone microenvironment, metastatic breast cancer cells hijack

*Corresponding Author: Dr. Conor C. Lynch, Department Of Orthopaedics and Rehabilitation, Vanderbilt University Medical Center East, South Tower, Suite 4200, Nashville, TN, 37232-8774. Tel: 615-343-5729. Fax: 615-343-1028. e-mail: conor.lynch@vanderbilt.edu.

the normal bone remodeling process to induce aberrant activation of bone resorbing osteoclasts (2). Increased bone resorption results in the release of sequestered growth factors from the bone matrix such as transforming growth factor β (TGFβ) and insulin like growth factors (IGFs). These factors subsequently promote tumor survival and growth thus completing what has aptly been described as the vicious cycle of tumor induced osteolysis (3).

Osteoclasts are critical for the completion of the vicious cycle since they are the principal cells involved in the direct resorption of the mineralized bone matrix. Therefore, understanding how osteoclast precursors are recruited to areas requiring bone remodeling and understanding the mechanisms involved in controlling their maturation and activation is key for the development of new therapies that can effectively stop the vicious cycle. In order to resorb bone, the osteoclast forms a resorptive seal on the mineralized bone matrix after retraction of the osteoblast canopy (4). Acidification of the resorption zone, in combination with collagenolysis, leads to the demineralization and degradation of the bone matrix respectively (5). Osteoclasts express a variety of proteases including the cysteine protease, cathepsin-K and matrix metalloproteinases (MMPs) (6). While cathepsin-K activity is critical for bone resorption (7), the role of osteoclast derived MMPs is less clear. The MMPs are a family of enzymatic proteins that are often overexpressed in the tumor microenvironment (8). Collectively, MMPs are capable of degrading the entire extracellular matrix (ECM) but more recently, MMPs have been implicated as important mediators of cell-cell communication by virtue of their ability to process multiple non-matrix molecules such as cytokines and growth factors to soluble forms resulting in either enhanced or attenuated activities (9).

In the context of the tumor-bone microenvironment, pre-clinical animals studies have demonstrated the efficacy of broad spectrum MMP inhibitors (MMPIs) in preventing tumor growth and tumor induced osteolysis (10-12). However, the failure of MMPIs in human clinical trials prevents their application for the treatment of bone metastases (13). A main conclusion derived from these trials was the necessity for defining the precise roles of individual MMPs in disease processes that would allow for the generation of highly selective MMP inhibitors. To this end, we have assessed the expression of MMPs in human clinical samples of osteolytic breast to bone metastasis. While the expression of many MMPs was noted throughout the tumor/stroma, MMP-7 and MMP-9 were highly localized to bone resorbing osteoclasts. Given the importance of the osteoclasts in driving the vicious cycle, the current study focused on determining if and how these osteoclast derived MMPs impacted tumor induced osteolysis.

Materials and Methods

Reagents

All experiments involving animals were conducted after review and approval by the office of animal welfare at Vanderbilt University. De-identified human samples of frank osteolytic breast to bone metastasis (n=11) were collected by curettage with IRB approval from Vanderbilt University from 2005 to 2008. Double null immunocompromised recombinase activating gene-2 (RAG-2) and MMP-7 mice were generated as previously described (14). Wild type and MMP-9 null mice in the FVB/N-Tg background were kindly provided by Dr. Lisa Coussens, Dept. of Pathology, University of California San Francisco. A luciferase expressing syngeneic FVB mammary tumor cell line derived from the polyoma virus middle T model of mammary tumorigenesis, designated PyMT-Luc, was isolated in our laboratory and maintained as previously described (15). A luciferase tagged 4T1 mammary tumor cell line (16) was kindly provided by Dr. Swati Biswas of the Vanderbilt Center for Bone Biology. All reagents were obtained from Sigma-Aldrich except where specified.

Intratibial injection and in vivo quantitation of tumor growth

PyMT-Luc and 4T1-Luc tumor cells (10^5) in a 10μl volume of sterile phosphate buffered saline (PBS) were injected into the tibia of anesthetized immunocompetent or immunocompromised 6 week old mice that were wild type or null for MMP-7 or MMP-9. The contralateral limb was injected with 10μl of PBS alone and acted as a sham injected control. The IVIS™ system (Caliper Life Sciences) was used to detect luminescence from PyMT-Luc and 4T1-Luc cells after intratibial injection. Firefly luciferin (120mg/kg in sterile PBS, Gold Biotechnology, Inc.) was delivered retro-orbitally 1 to 2 minutes prior imaging. Mice were imaged at 24 hours and every 3 days after surgery until day 9 which was previously determined to be the time point prior to tumor breach of the cortical bone in wild type control mice. Living Image™ software (Calipers Life Sciences) was used to quantify the luminescence intensity in the tumor bearing limb over time. Mice were sacrificed at 9 days post-surgery and both the tumor injected and contralateral control tibiae were harvested. All animal studies were independently repeated at least twice.

Histology

Fresh human breast-to-bone metastases, tumor and sham injected mouse tibiae were fixed overnight in 10% buffered formalin and decalcified for 3 weeks in 14% EDTA at pH 7.4 with changes every 48-72 hours. Tissues were embedded in paraffin and 5μm thick sections were cut. For MMP-7, MMP-9 and tartrate resistant acid phosphatase (TRAcP) localization, the following technique was employed. Sections were rehydrated through a series of ethanols and then rinsed in tris buffered saline (TBS; 10mM Tris at pH 7.4, 150mM NaCl) with Tween-20 (0.05%). For antigen retrieval, slides were immersed in a 20μg/ml solution of proteinase K according to the manufacturer's instructions for 10 minutes at room temperature. Following washing in TBS, tissue sections were blocked using standard blocking criteria for 1 hour at room temperature. MMP-7 (17) or MMP-9 (Oncogene, Cat. No. AB3-IM37L) antibodies at a dilution of 1:100 were added in blocking solution overnight at 4°C. Slides were washed extensively in TBST prior to the addition of a species specific fluorescently labeled secondary antibody (Alexafluor 568nm, Invitrogen) diluted 1:1,000 in blocking solution for 1 hour at room temperature. Slides were washed in TBS and then equilibrated in an acetate buffer as described (18). The ELF97 TRAcP stain (Invitrogen, Cat. No. 6601) was diluted 1:1,000 in acetate buffer and slides were incubated for 15 minutes at room temperature. Following washing, slides were aqueously mounted in media (Biomeda Corp) containing 2μM DAPI (4′, 6 diamidino-2-phenylindole) for nuclear localization.

TRAcP was also detected using a traditional colorimetric kit according to the manufacturer's instructions (Sigma-Aldrich, Cat. No. 387A). Gross anatomy of the mouse tibiae was assessed by hematoxylin and eosin (H&E) staining. Proliferation (anti-phospho Histone H3, Millipore, Cat. No. 06-570) and apoptosis (anti-Caspase-3, Cell Signaling, Cat. No. 9662) were assessed by immunohistochemistry as previously described (14).

Micro computed tomography (μCT), X-ray and histomorphometric analyses

For gross analysis of trabecular bone volume, formalin fixed tibiae were scanned at an isotropic voxel size of 12μm using a microCT40 (SCANCO Medical). The tissue volume (TV) was derived from generating a contour around the metaphyseal trabecular bone that excluded the cortices. The area of measurement began at least 0.2mm below the growth plate and was extended by 0.12mm. The bone volume (BV) included all bone tissue that had a material density greater than 438.7 mgHA/cm^3. These analyses allowed for the calculation of the BV/TV ratio. The same threshold setting for bone tissue was used for all samples. Radiographic images (Faxitron X-ray Corp) were obtained using an energy of 35kV and an exposure time of 8 seconds. The tumor volume (TuV) was calculated as a function of the total tissue volume (TV) of the tibial medullary canal using Metamorph® software (Molecular Devices). For

histomorphometry, three non-serial sections of tumor bearing limbs were H&E stained to assess the ratio of BV/TV or with TRAcP to assess osteoclast number per mm of bone at the tumor-bone interface using Metamorph®.

Immunoprecipitation, immunoblotting and ELISA

Tumor and sham injected tibias from wild type or MMP null animals were harvested 9 days post-injection and flash frozen in liquid nitrogen. Tissue homogenates were generated by mortar and pestle and total protein was subsequently extracted using a standard protein lysis buffer containing a complete protease inhibitor cocktail (Roche, Cat. No. 11836145001). Protein concentration in isolated samples was quantitated using a bicinchoninic acid (BCA) assay as per manufacturer's instructions (Pierce, Cat. No. 23227). For immunoprecipitation and quantitation of soluble RANKL in the tumor bone microenvironments, equal concentrations of total protein (1mg) in 1ml of PBS were pre-cleared with 10μl of protein-G-sepharose beads (Amersham Biosciences) for one hour at 4°C. Pre-cleared lysates were then incubated with 2μg of antibody directed to the N-terminus of RANKL (sc-7628, Santa Cruz Biotechnology) for 1 hour at 4°C. Subsequently, 10μl of protein G-sepharose beads were added to the samples and the bead-antibody-protein complexes were allowed to form overnight at 4° C. A nutator was used during all steps for agitation. The complexes were washed extensively (100mM NaCl, 50mM Tris-HCl, pH7.5, 0.5% NP-40) and then boiled in sample buffer (10% SDS, 0.5M Tris-HCl pH 6.8, 30% glycerol, 1% β-mercaptoethanol and 0.02% bromophenol blue) for 10 minutes prior to loading on to a 15% SDS-PAGE gel. Recombinant RANKL (462-TR-010/CF, RnD Systems) or MMP-7 solubilized RANKL (10μg recombinant RANKL incubated with 100ng active MMP-7 (cat # 444270, Calbiochem) for 1 hour at 37°C as previously described (14)) were added as positive controls for the molecular weight of full length and MMP solubilized RANKL. Proteins were transferred to nitrocellulose membranes and blocked for 1 hour at room temperature (5% milk powder in 1×TBS). The blots were then panned with an antibody directed to the N-terminus of RANKL (1: 1,000 dilution; Cat # 804-243-C100, Axxora LLC in 5% milk in 1×TBST) overnight with rocking at 4°C. The following day, blots were washed extensively with 1×TBST prior to the addition of a secondary infra-red labeled anti-mouse antibody (1: 5,000 dilution in 1×TBST-Cat# 610-132-121, Rockland Inc.) for 1 hour at room temperature. After washing in 1×TBST, blots were developed and bands of interest were quantitated using the Odyssey system (LI-COR Biosciences). ELISA was also used for the quantitation of soluble RANKL in samples according to the manufacturer's instructions (Quantikine, R&D Systems, Cat. No. MTR00).

Statistical analyses

For *in vivo* data, statistical analysis was performed using Anova and Bonferroni multiple comparison tests. *In vitro*, statistical significance was analyzed using a student's t test. A value of $p < 0.05$ was considered significant. Data are presented as mean ± standard deviation (SD).

Results

MMP-7 and MMP-9 are expressed by osteoclasts in human breast to bone metastases

Previous observations using an animal model of tumor-bone interaction identified several MMPs as being highly expressed at the tumor-bone interface compared to the tumor area alone, namely MMP-2, -3, -7, -9 and -13 ((14) and unpublished observations). The expression of these MMPs was examined in human cases of frank breast to bone metastasis (n=11). Interestingly, MMP-7 and MMP-9 were largely localized to the majority of mature TRAcP positive multinucleated osteoclasts at the tumor-bone interface in human samples containing areas of osteolysis (10 of 11 samples) (Fig. 1A-C and supplemental Fig. S1 and S2). Other cells in the stromal compartment stained positively for MMP-7 and MMP-9 but remarkably, the tumor cells were negative for these metalloproteinases. MMP-2, -3 and -13 were also detected but

their expression was diffuse throughout the tumor/stroma compartment (data not shown). Since osteoclasts are the principal cells involved in bone resorption, we examined whether the ablation of host derived MMP-7 or MMP-9 would impact the vicious cycle in terms of mammary tumor growth and/or mammary tumor induced osteolysis.

Host derived MMP-9 does not contribute to tumor growth or tumor induced osteolysis

MMP-9 has previously been reported to be localized to osteoclasts and MMP-9 null animals have been identified as having a delay in osteoclast recruitment during the development of long bones (19). Therefore, we initially tested the role of host derived MMP-9 in tumor growth or tumor induced osteolysis. Consistent with our observations in human samples, bone resorbing osteoclasts in wild type mice were positive for MMP-9 expression by immunofluorescent staining while as expected, MMP-9 was not detected in MMP-9 null osteoclasts (Fig. 2A). Since MMP-9 null animals have a transient developmental bone phenotype, we determined the baseline trabecular bone volume as a function of tissue volume (BV/TV) in wild type and MMP-9 null animals at 6 weeks of age which was the proposed time-point for introduction of the PyMT-Luc tumor cells. No difference in the BV/TV between the wild-type and MMP-9 null animals was observed (Fig. S3A).

To assess the contribution of host MMP-9 in mammary tumor growth in the bone microenvironment, the PyMT-Luc tumor cells, in which MMP-9 expression is undetectable *in vivo* (20), were injected into the tibia of syngeneic FVB wild-type or MMP-9 null mice. Surprisingly, quantitation of the bioluminescent signal from the tumor cells showed no difference in the tumor growth rate between the MMP-9 null and wild type control mice (Fig. 2B). With respect to tumor induced osteolysis, analysis of the BV/TV ratio by high resolution μCT demonstrated that the tumor injected tibias of wild-type and MMP-9 null were significantly lower ($p<0.05$) than their respective sham injected control counterparts (Fig. 2C). However, a direct comparison of the BV/TV ratios between the wild-type and MMP-9 null tumor injected limbs revealed no difference in BV/TV ratios (Fig. 2C). Furthermore, no differences in tumor growth as assessed by phospho histone H3 for proliferation and cleaved caspase-3 immunohistochemistry for apoptosis, trabecular bone volume and osteoclasts/mm bone by histomorphometry were observed between the wild type and MMP-9 null groups (data not shown). These experiments, with similar sized groups were repeated on several occasions with similar results. These results using the intratibial model suggest that host MMP-9 does not contribute to mammary tumor growth in the bone or tumor induced osteolysis and are consistent with studies examining the role of host MMP-9 in the prostate cancer-bone microenvironment (21).

Host MMP-7 contributes to mammary tumor growth in the bone microenvironment

This is the first report to document the expression of MMP-7 in human breast to bone metastases and in human osteoclasts (Fig. 1), although MMP-7 has previously been identified in rodent osteoclasts by our group (14). Recapitulating observations in human clinical samples, MMP-7 expression was identified in wild type murine osteoclasts and not in MMP-7 null osteoclasts (Fig. 3A). Given that MMP-7 expression by osteoclasts is a relatively recent observation, studies into defining roles for MMP-7 in skeletal development have not been explored thus far. Therefore, prior to testing the impact of host derived MMP-7 on the vicious cycle, the trabecular bone volume in non-injected, 6 week old immunocompromised wild type and MMP-7 null animals was examined using high resolution μCT. Our results revealed no significant difference in the BV/TV ratio between wild type and MMP-7 null animals suggesting that at this time point, MMP-7 null animals do not display an obvious bone phenotype in comparison to the wild type controls (Fig. S3B).

To determine the contribution of host MMP-7 to mammary tumor growth in the bone microenvironment, PyMT-Luc cells were injected into 6 week old wild-type or MMP-7 null mice. Quantitation of the bioluminescent signal from the PyMT-Luc cells demonstrated a significant decrease in the tumor growth rate in MMP-7 null mice compared to the wild type controls (Fig. 3B). These experiments with similar sized groups in terms of animal numbers were independently repeated on four occasions and similar observations were noted. To further investigate the potential role of MMP-7 in tumor growth, tumor proliferation and apoptosis were assessed by immunohistochemistry for phospho-histone H3 and cleaved caspase-3, respectively, in multiple sections from at least five animals per group (Fig. 3C and D). Surprisingly, no difference in tumor proliferation was observed between the wild type and MMP-7 null groups, however, tumor apoptosis was significantly higher in MMP-7 null mice compared to the wild type controls ($p<0.05$). Similar findings with respect to the impact of host MMP-7 on tumor growth using the 4T1-Luc cell line were also observed (Fig. S4A-C). These results suggest that host-derived MMP-7 significantly contributes to mammary tumor growth in the bone by enhancing tumor cell survival.

Host derived MMP-7 contributes to mammary tumor induced osteolysis

The vicious cycle of tumor-bone interaction suggests that tumor growth/survival is dependent on osteoclast mediated bone resorption. Since MMP-7 is primarily localized to bone resorbing osteoclasts in the tumor-bone microenvironment, we assessed whether a lack of MMP-7 in osteoclasts impacted tumor induced osteolysis. Analysis of the BV/TV ratios from wild type and MMP-7 null tumor injected tibias using μCT (Fig. 4A) and histomorphometry (Fig. 4B) revealed that the MMP-7 null group had a significantly higher amount of trabecular bone which is in keeping with our tumor growth data, i.e. less tumor growth in the MMP-7 null animal would lead to less osteolysis. X-ray analysis also revealed a significantly lower tumor volume in the MMP-7 null animals compared to wild type controls (Fig. 4C). Studies using the 4T1-Luc cell line also demonstrated that host derived MMP-7 also significantly impacted tumor induced osteolysis (Figure S5A and B). These results demonstrate that host derived MMP-7 significantly impacts mammary tumor induced osteolysis.

MMP-7 mediates RANKL solubilization in the tumor-bone microenvironment

Next, we explored the potential molecular mechanism through which osteoclast derived MMP-7 was impacting tumor induced osteolysis. Given the acidity of the resorption lacunae ($pH<4$) and the neutral activity profile of MMP-7, we suggest that MMP-7 does not function in direct bone matrix degradation but in the processing of factors that impact cell-cell communication within the tumor-bone microenvironment. MMP-7 has previously been shown to process a number of growth factors and cytokines to soluble active forms including members of the tumor necrosis factor family (TNF), TNF-α, Fas ligand (FasL) and RANKL (14,22, 23). RANKL is essential for osteoclastogenesis and is a potent chemotactic molecule for monocytes and osteoclast precursor cells (24,25). Therefore, we investigated if MMP-7 solubilization of RANKL was relevant in our model.

ELISA analysis revealed lower levels of total RANKL (membrane bound and soluble) in the tumor injected tibias of MMP-7 null mice compared to wild type control mice (Fig. 5A) while no difference was observed in the sham injected control counterparts of each group (data not shown). Similar levels of osteoprotegerin (OPG), a soluble decoy receptor of RANKL, were found in the wild-type and MMP-7 null animals and were not present at a high enough concentration to interfere with the detection of RANKL by ELISA (data not shown). Immunoprecipitation and immunoblotting for soluble RANKL revealed significantly lower levels of soluble RANKL in PyMT-Luc or 4T1-Luc tumor injected MMP-7 null animals compared to wild type controls as assessed by densitometry (Fig. 5B; $p<0.05$ and Fig S5C; $p<0.05$).

Interestingly, soluble RANKL could still be detected in the tumor bearing limbs of MMP-7 null animals. This suggests that RANKL solubilization is still occurring in the absence of MMP-7. We and others have previously identified that other metalloproteinases such as MMP-1, -3, -14, a disintegrin and metalloprotease-17 (ADAM-17) and the serine protease cathepsin G are capable of processing RANKL to a soluble active form and therefore, these proteases may also be playing a role in the solubilization of RANKL in our model (14, 26-28). However, since the levels of RANKL are significantly lower in the MMP-7 null mice, we suggest that MMP-7 is the dominant protease involved in RANKL solubilization.

Next, since a decrease in the amount of soluble RANKL was detected in the tumor bearing limbs of the MMP-7 null animals, we asked if there was concomitant decrease in the number of osteoclasts in the MMP-7 null tumor-bone microenvironment. We observed significantly lower numbers of TRAcP positive multinucleated osteoclasts per unit length of tumor-bone interface in the MMP-7 null animals compared to the wild-type controls (Fig. 5C). Significantly lower numbers of osteoclasts were also recorded in MMP-7 deficient animals injected with 4T1-Luc cells compared to wild type controls (Fig. S5D). Given the importance of RANKL in mediating osteoclastogenesis, these data suggest that MMP-7 mediates mammary tumor induced osteolysis by impacting the availability of a key factor for osteoclastogenesis, RANKL.

Discussion

Understanding the molecular mechanisms that control the vicious cycle is key for the development of new therapeutics that will be effective not only in treating bone metastases but also in curing them. In the current study, we found that in human cases of breast to bone metastasis, osteoclasts were a rich source of MMP-7 and MMP-9. Interestingly, our studies using two unrelated osteolytic inducing tumor cell lines (PyMT-Luc and 4T1-Luc) revealed that only MMP-7 appeared to contribute to mammary tumor growth and tumor induced osteolysis in the bone microenvironment. Furthermore, our data suggests that MMP-7 solubilization of the osteoclastogenic factor RANKL is the principal molecular mechanism underlying these observations. Previously, we have identified that MMP-7 processing of RANKL results in the generation of an active soluble form that can promote osteoclast maturation and activation (14). Therefore, in the context of breast to bone metastasis, we hypothesize that in the absence of MMP-7 solubilized RANKL, there is a resultant decrease in osteoclast maturation and bone resorption at the tumor-bone interface that in turn results in a decrease in bone derived growth factors such as TGFβ and IGF that impact tumor survival and growth (Fig. 6).

Our results show an osteoclast derived protease, MMP-7, can promote osteoclast activation in the tumor-bone microenvironment by generating an active soluble form of the osteoclastogenic factor, RANKL and suggest that selective inhibition of MMP-7 may be of benefit for the treatment of lytic metastases. Several studies support the rationale for the development of selective MMP inhibitors for the treatment of bone metastases. Broad spectrum MMP inhibitors such as batimastat have been identified as being effective in preventing tumor growth and tumor induced osteolysis in the bone environment using animal models (10-12). However, conclusions from human clinical trials with the same inhibitors identified the necessity for highly selective MMPIs that lack the deleterious side effects of broad spectrum inhibitors prior to their application in clinical settings (13). This requires an understanding of the precise roles of MMPs in the context of particular diseases and in this regard, our studies suggest MMP-7 as an attractive target for the treatment of lytic metastases.

While MMP-7 solubilization of RANKL is predicted here to be a mechanism underlying our observations, MMP-7 may contribute via other mechanisms. For example, MMP-7 processing of apoptotic factors such as Fas ligand in the tumor-bone microenvironment may directly

impact tumor survival (22). In addition, the direct processing of the bone matrix by MMP-7 may also be a possibility. Acidification and cathepsin-K secretion into osteoclast resorption lacunae allows for the demineralization and collagenolysis of the bone matrix respectively (6). By a process known as transcytosis, the osteoclast mediates the removal of bone products from the area of bone undergoing resorption (29). Given the punctate localization of MMP-7 by immunofluorescent staining (Fig. 1A and 3A) it is tempting to speculate that MMP-7 contributes to the further processing of bone matrix components such as osteopontin (30), or the release of growth factors from bone matrix components such as TGFβ (31) and IGFs (32), within these transcytotic vesicles. The expression of MMP-7 from other cellular sources may also be a possibility. In the tumor-bone microenvironment, we observed that MMP-7 expression was largely confined to osteoclasts. However, MMP-7 has also been shown to be expressed by macrophages and given the role of macrophages in tumor induced osteolysis, the contribution of macrophage derived MMP-7 in our model or in humans cannot be discounted (33,34).

Given the apparent role of MMP-7 in osteoclast function in the pathological setting of tumor induced osteolysis, it is surprising that MMP-7 null animals appear to have a normal skeletal phenotype. Data presented here using μCT scan analysis demonstrate a similar BV/TV ratio between MMP-7 null and wild type control mice at 6 weeks of age. While a role for MMP-7 in bone development has not been explored, a number of reports have revealed that the phenotype of the MMP-7 null animals often becomes apparent in response to injury/challenges or disease. For example, in non-pathological conditions such as herniated disc resorption, macrophage derived MMP-7 is critical for the resorption of the herniated disc and in mammary and prostate involution, MMP-7 processing of FasL is important for initiating apoptosis (22, 23,35). More often, phenotypes in the MMP-7 null animals have been observed in pathological conditions such as pancreatitis, colon tumorigenesis, mammary gland tumorigenesis and in innate defense wherein MMP-7 null animals show significant delays in disease progression or in response to infection (36-39). Therefore, although MMP-7 null mice lack an apparent skeletal phenotype, in the context of tumor-bone microenvironment, it is clear based on the results in the current study that host MMP-7 plays an important role in osteoclast biology. In addition, our observations defining a role for MMP-7 in bone diseases are consistent with previous reports that implicate roles for host MMP-7 in prostate cancer induced osteolysis, osteoarthritis and cartilage/periarticular bone destruction (14,40,41).

Although MMP-9 was localized to human and murine osteoclasts, the ablation of host MMP-9 did not appear to impact PyMT-Luc tumor growth and bone resorption compared to the wild-type controls. Analogous results were obtained by Nabha et al., using the same intratibial model but in the context of prostate cancer progression in the bone (21). Given the importance of MMP-9 in osteoclast migration and recruitment in developing long bones (19), these results were surprising. It appears that in the tumor-bone microenvironment, MMP-9 is not critical for osteoclast function. The possibility that tumor-derived MMP-9 could overcome the absence of host MMP-9 exists in our model, however, *in vivo* studies by our group have demonstrated that MMP-9 expression by the PyMT-Luc tumor cells is not detectable (20). Therefore, the ability of tumor derived MMP-9 to circumvent the loss of host derived MMP-9 and impact tumor progression in the bone is unlikely. However, due to functional overlap amongst members of the MMP family, other MMPs produced by osteoclasts and other stromal cells in the tumor microenvironment may compensate for the absence of host MMP-9.

While our data points towards MMP-9 as not being critical for mammary tumor growth or induced osteolysis, it is important to note that MMP-9 could contribute to other steps of metastasis that are not taken into account with the intratibial model. These include extravasation from the sinusoidal vasculature in the bone and initial survival, the latter of which has been shown to be an important role for host derived MMP-9 in early lung metastasis (42).

Furthermore, MMP-9 has been implicated in tumor angiogenesis by mediating the release of matrix sequestered vascular endothelial growth factor (VEGF) (43). In the context of the prostate tumor-bone microenvironment, Nabha and colleagues demonstrated a decrease in angiogenesis in MMP-9 null animals compared to wild type controls (21). Therefore, the selective inhibition of MMP-9 may still prove useful in preventing the establishment and angiogenesis of bone metastases.

In conclusion, this study demonstrates that osteoclast derived MMP-7, but not MMP-9, significantly contributes to tumor induced osteolysis by impacting osteoclast activation. We suggest that MMP-7 mediated solubilization of RANKL is a potential mechanism underlying this observation. Our data supports the rationale for the generation of selective MMP inhibitors for the treatment of osteolytic bone metastases and implies that the development of such reagents would expand the therapeutic options available to patients suffering with this incurable disease.

Supplementary Material

Refer to Web version on PubMed Central for supplementary material.

Acknowledgments

We would like to thank James Edwards and Steve Munoz of the Vanderbilt Bone Center for their expertise. This research was supported by NIH: 1 R01 CA84360 (LMM) and Susan G. Komen Foundation: PDF 02 1394 (CCL) CCL and ST are supported by the Department of Defense under award number W81XWH-07-1-0208 and BC051038 respectively. Views and opinions of, and endorsements by the author(s) do not reflect those of the US Army or the Department of Defense.

References

1. Coleman RE, Rubens RD. The clinical course of bone metastases from breast cancer. British Journal of Cancer 1987;55:61–6. [PubMed: 3814476]
2. Mundy GR. Metastasis to bone: causes, consequences and therapeutic opportunities. Nature Reviews Cancer 2002;2:584–93.
3. Chirgwin JM, Guise TA. Molecular mechanisms of tumor-bone interactions in osteolytic metastases. Crit RevEukaryotGene Expr 2000;10:159–78.
4. Compston JE. Bone marrow and bone: a functional unit. J Endocrinol 2002;173:387–94. [PubMed: 12065228]
5. Delaisse JM, Engsig MT, Everts V, et al. Proteinases in bone resorption: obvious and less obvious roles. Clinica Chimica Acta 2000;291:223–34.
6. Delaisse JM, Andersen TL, Engsig MT, Henriksen K, Troen T, Blavier L. Matrix metalloproteinases (MMP) and cathepsin K contribute differently to osteoclastic activities. Microscopy Research and Technique 2003;61:504–13. [PubMed: 12879418]
7. Saftig P, Hunziker E, Wehmeyer O, et al. Impaired osteoclastic bone resorption leads to osteopetrosis in cathepsin-K-deficient mice. Proc Natl Acad Sci U S A 1998;95:13453–8. [PubMed: 9811821]
8. Chambers AF, Matrisian LM. Changing views of the role of matrix metalloproteinases in metastasis. Journal National Cancer Institute 1997;89:1260–70.
9. Lynch CC, Matrisian LM. Matrix metalloproteinases in tumor-host cell communication. Differentiation 2002;70:561–73. [PubMed: 12492497]
10. Lee J, Weber M, Mejia S, Bone E, Watson P, Orr W. A matrix metalloproteinase inhibitor, batimastat, retards the development of osteolytic bone metastases by MDA-MB-231 human breast cancer cells in Balb C nu/nu mice. European Journal of Cancer 2001;37:106–13. [PubMed: 11165137]
11. Winding B, NicAmhlaoibh R, Misander H, et al. Synthetic matrix metalloproteinase inhibitors inhibit growth of established breast cancer osteolytic lesions and prolong survival in mice. Clinical Cancer Research 2002;8:1932–9. [PubMed: 12060638]

12. Nemeth JA, Yousif R, Herzog M, et al. Matrix metalloproteinase activity, bone matrix turnover, and tumor cell proliferation in prostate cancer bone metastasis. Journal National Cancer Institute 2002;94:17–25.

13. Coussens LM, Fingleton B, Matrisian LM. Matrix metalloproteinase inhibitors and cancer: trials and tribulations. Science 2002;295:2387–92. [PubMed: 11923519]

14. Lynch CC, Hikosaka A, Acuff HB, et al. MMP-7 promotes prostate cancer-induced osteolysis via the solubilization of RANKL. Cancer Cell 2005;7:485–96. [PubMed: 15894268]

15. Halpern J, Lynch CC, Fleming J, et al. The application of a murine bone bioreactor as a model of tumor: bone interaction. Clin Exp Metastasis 2006;23:345–56. [PubMed: 17136574]

16. Aslakson CJ, Miller FR. Selective events in the metastatic process defined by analysis of the sequential dissemination of subpopulations of a mouse mammary tumor. Cancer Res 1992;52:1399–405. [PubMed: 1540948]

17. Fingleton B, Powell WC, Crawford HC, Couchman JR, Matrisian LM. A rat monoclonal antibody that recognizes pro- and active MMP-7 indicates polarized expression in vivo. Hybridoma (Larchmt) 2007;26:22–7. [PubMed: 17316082]

18. Filgueira L. Fluorescence-based staining for tartrate-resistant acidic phosphatase (TRAP) in osteoclasts combined with other fluorescent dyes and protocols. J Histochem Cytochem 2004;52:411–4. [PubMed: 14966208]

19. Engsig MT, Chen QJ, Vu TH, et al. Matrix metalloproteinase 9 and vascular endothelial growth factor are essential for osteoclast recruitment into developing long bones. Journal of Cell Biology 2000;151:879–90. [PubMed: 11076971]

20. Martin M, Carter K, Thiolloy S, Lynch CC, Matrisian L, Fingleton B. Effect of ablation or inhibition of stromal matrix metalloproteinase-9 on lung metastasis in a breast cancer model is dependent on genetic background. Cancer Res 2008;68E-Pub ahead of print

21. Nabha SM, Bonfil RD, Yamamoto HA, et al. Host matrix metalloproteinase-9 contributes to tumor vascularization without affecting tumor growth in a model of prostate cancer bone metastasis. Clin Exp Metastasis 2006;23:335–44. [PubMed: 17136575]

22. Powell WC, Fingleton B, Wilson CL, Boothby M, Matrisian LM. The metalloproteinase matrilysin (MMP-7) proteolytically generates active soluble Fas ligand and potentiates epithelial cell apoptosis. Current Biology 1999;9:1441–7. [PubMed: 10607586]

23. Haro H, Crawford HC, Fingleton B, Shinomiya K, Spengler DM, Matrisian LM. Matrix metalloproteinase-7-dependent release of tumor necrosis factor-alpha in a model of herniated disc resorption. Journal of Clinical Investigation 2000;105:143–50. [PubMed: 10642592]

24. Kong YY, Yoshida H, Sarosi I, et al. OPGL is a key regulator of osteoclastogenesis, lymphocyte development and lymph-node organogenesis. Nature 1999;397:315–23. [PubMed: 9950424]

25. Breuil V, Schmid-Antomarchi H, Schmid-Alliana A, Rezzonico R, Euller-Ziegler L, Rossi B. The receptor activator of nuclear factor (NF)-kappaB ligand (RANKL) is a new chemotactic factor for human monocytes. Faseb J 2003;17:1751–3. [PubMed: 12958198]

26. Lum L, Wong BR, Josien R, et al. Evidence for a role of a tumor necrosis factor-alpha (TNF-alpha)-converting enzyme-like protease in shedding of TRANCE, a TNF family member involved in osteoclastogenesis and dendritic cell survival. J Biol Chem 1999;274:13613–8. [PubMed: 10224132]

27. Schlondorff J, Lum L, Blobel CP. Biochemical and pharmacological criteria define two shedding activities for TRANCE/OPGL that are distinct from the tumor necrosis factor alpha convertase. J Biol Chem 2001;276:14665–74. [PubMed: 11278735]

28. Wilson TJ, Nannuru KC, Futakuchi M, Sadanandam A, Singh RK. Cathepsin G enhances mammary tumor-induced osteolysis by generating soluble receptor activator of nuclear factor-kappaB ligand. Cancer Res 2008;68:5803–11. [PubMed: 18632634]

29. Blair HC. How the osteoclast degrades bone. Bioessays 1998;20:837–46. [PubMed: 9819571]

30. Agnihotri R, Crawford HC, Haro H, Matrisian LM, Havrda MC, Liaw L. Osteopontin, a novel substrate for matrix metalloproteinase-3 (stromelysin-1) and matrix metalloproteinase-7 (matrilysin). Journal Biological Chemistry 2001;276:28261–7.

31. Imai K, Hiramatsu A, Fukushima D, Pierschbacher MD, Okada Y. Degradation of decorin by matrix metalloproteinases: identification of the cleavage sites, kinetic analyses and transforming growth factor-beta 1 release. Biochemical Journal 1997;322:809–14. [PubMed: 9148753]

32. Miyamoto S, Yano K, Sugimoto S, et al. Matrix metalloproteinase-7 facilitates insulin-like growth factor bioavailability through its proteinase activity on insulin-like growth factor binding protein 3. Cancer Research 2004;64:665–71. [PubMed: 14744783]
33. Burke B, Giannoudis A, Corke KP, et al. Hypoxia-induced gene expression in human macrophages: implications for ischemic tissues and hypoxia-regulated gene therapy. American Journal of Pathology 2003;163:1233–43. [PubMed: 14507633]
34. Athanasou NA, Sabokbar A. Human osteoclast ontogeny and pathological bone resorption. Histol Histopathol 1999;14:635–47. [PubMed: 10212824]
35. Fingleton B, Vargo-Gogola T, Crawford HC, Matrisian LM. Matrilysin [MMP-7] expression selects for cells with reduced sensitivity to apoptosis. Neoplasia 2001;3:459–68. [PubMed: 11774028]
36. Sawey ET, Johnson JA, Crawford HC. Matrix metalloproteinase 7 controls pancreatic acinar cell transdifferentiation by activating the Notch signaling pathway. Proc Natl Acad Sci U S A 2007;104:19327–32. [PubMed: 18042722]
37. Wilson CL, Heppner KJ, Labosky PA, Hogan BL, Matrisian LM. Intestinal tumorigenesis is suppressed in mice lacking the metalloproteinase matrilysin. Proc Natl Acad Sci U S A 1997;94:1402–7. [PubMed: 9037065]
38. Wilson CL, Ouellette AJ, Satchell DP, et al. Regulation of intestinal alpha-defensin activation by the metalloproteinase matrilysin in innate host defense. Science 1999;286:113–7. [PubMed: 10506557]
39. Rudolph-Owen LA, Matrisian LM. Matrix metalloproteinases in remodeling of the normal and neoplastic mammary gland. J Mammary Gland Biol Neoplasia 1998;3:177–89. [PubMed: 10819526]
40. Gjertsson I, Innocenti M, Matrisian LM, Tarkowski A. Metalloproteinase-7 contributes to joint destruction in Staphylococcus aureus induced arthritis. Microb Pathog 2005;38:97–105. [PubMed: 15748811]
41. Ohta S, Imai K, Yamashita K, Matsumoto T, Azumano I, Okada Y. Expression of matrix metalloproteinase 7 (matrilysin) in human osteoarthritic cartilage. Laboratory Investigation 1998;78:79–87. [PubMed: 9461124]
42. Acuff HB, Carter KJ, Fingleton B, Gorden DL, Matrisian LM. Matrix metalloproteinase-9 from bone marrow-derived cells contributes to survival but not growth of tumor cells in the lung microenvironment 1. Cancer Research 2006;66:259–66. [PubMed: 16397239]
43. Bergers G, Brekken R, McMahon G, et al. Matrix metalloproteinase-9 triggers the angiogenic switch during carcinogenesis. Nature Cell Biology 2000;2:737–44.

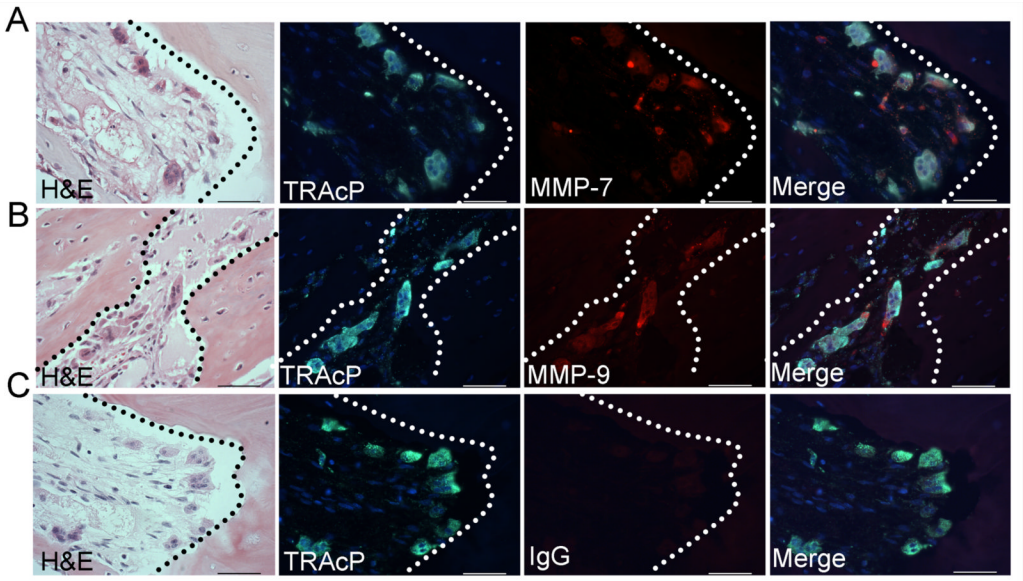

Figure 1.

MMP-7 and MMP-9 localization in human breast to bone metastases (n=11). **A**-**C**: Fluorescent TRAcP staining (green) was used to localize osteoclasts (arrows) while immunofluorescence was used to localize MMP-7 and MMP-9 (red). DAPI (blue) was used as a nuclear stain. Murine or rat IgG was used as a negative control. Dashed line represents the tumor-bone interface. Scale bars are 50μm.

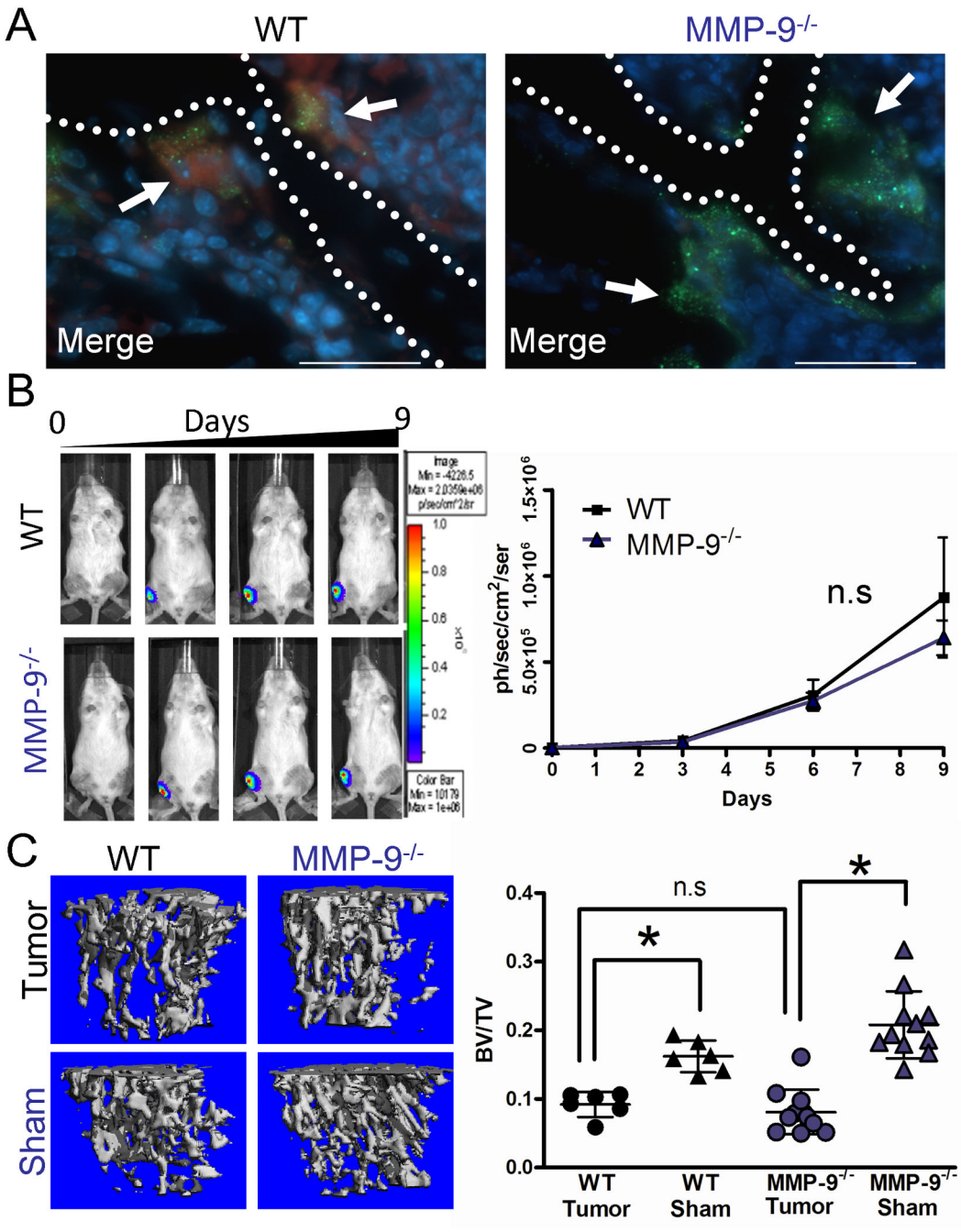

Figure 2.

Host MMP-9 does not impact mammary tumor growth or osteolysis in the bone microenvironment. **A**: Representative photomicrographs of MMP-9 (red) localization merged with TRAcP (green) localization in WT and MMP-9$^{-/-}$ animals. DAPI (blue) was used as a nuclear stain. Arrows indicate osteoclasts while dashed line represents the tumor-bone interface. Scale bars are 50μm. **B**: PyMT-Luc cells were injected intratibially into syngeneic FVB wild type (WT; n=6) or MMP-9 null (MMP-9$^{-/-}$; n=11). The contralateral limb received a sham injection of saline. Luciferase activity was measured over a 9 day period and used to quantitate tumor growth. **C**: Representative μCT scans of trabecular bone from tumor bearing and sham injected limbs of WT and MMP-9$^{-/-}$ animals. μCT was also used to calculate the

ratio of trabecular bone volume to tissue volume (BV/TV) for tumor injected and sham injected wild type and MMP-9$^{-/-}$ mice. Data are mean ± SD. Asterisk denotes that $p<0.05$ while n.s. indicates a non-significant p value.

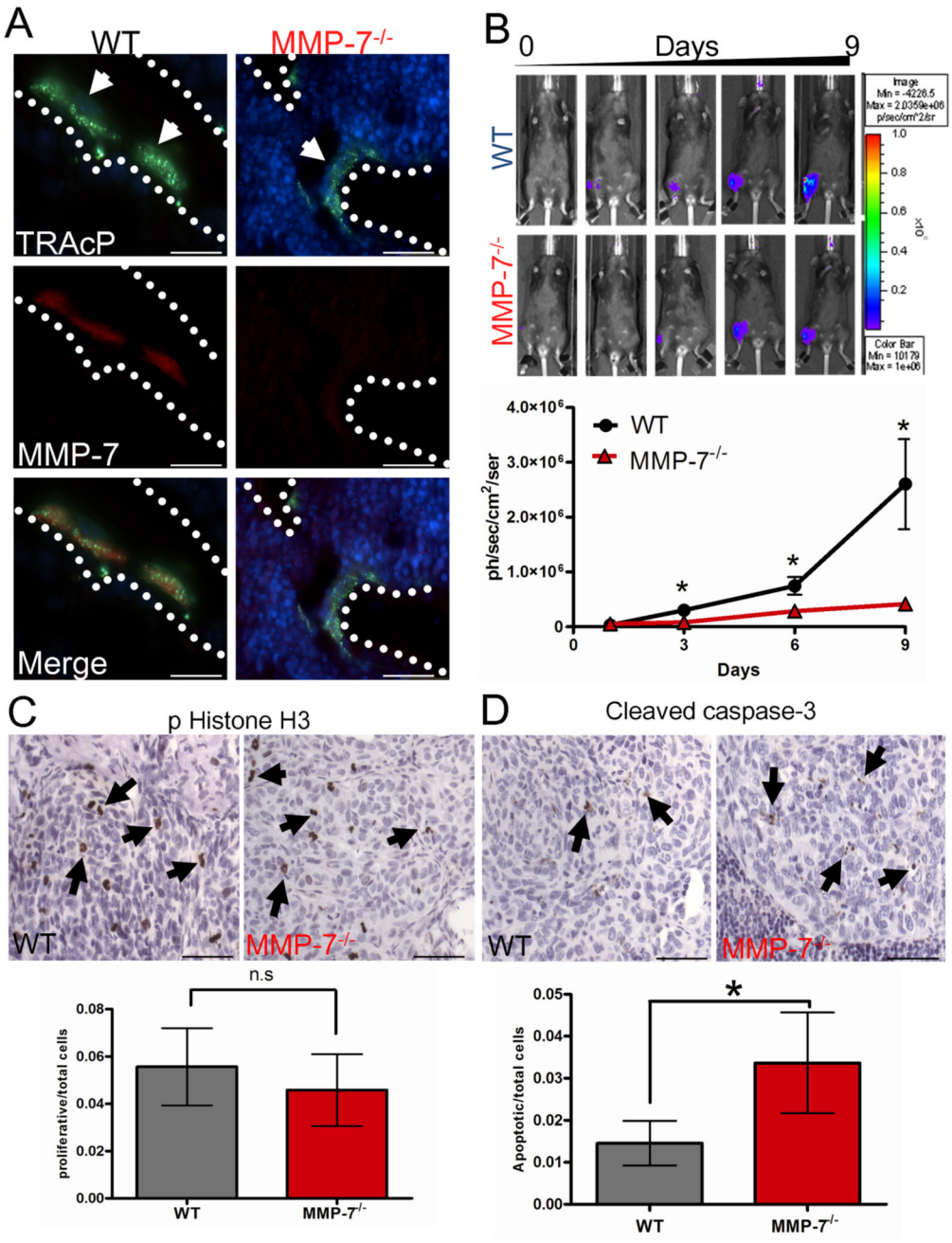

Figure 3.

Host MMP-7 contributes to mammary tumor growth in the bone microenvironment. **A**: Representative photomicrographs of MMP-7 (red) immunofluorescent localization merged with TRAcP (green) localization in WT and MMP-7$^{-/-}$ animals. DAPI (blue) was used as nuclear stain. Arrows indicate osteoclasts while dashed line represents the tumor-bone interface. **B**: PyMT-Luc cells were injected intratibially into RAG-2 null (WT; n=5) or MMP-7 null (MMP-7$^{-/-}$; n=10). The contralateral limb received a sham injection of saline. Luciferase activity was determined over a nine day period and used as a measure of tumor growth. **C**-**D**: Proliferative or apoptotic cells (arrows) in representative sections of WT and MMP-7$^{-/-}$ injected tibias were identified by immunostaining of phospho Histone H3 (pHistone H3) or cleaved

caspase-3 respectively. The number of positively stained cells per total number of cells was calculated. Scale bars represent 50 μm in all photomicrographs. Data are mean ± SD. Asterisk denotes that $p<0.05$ while n.s. indicates a non-significant p value.

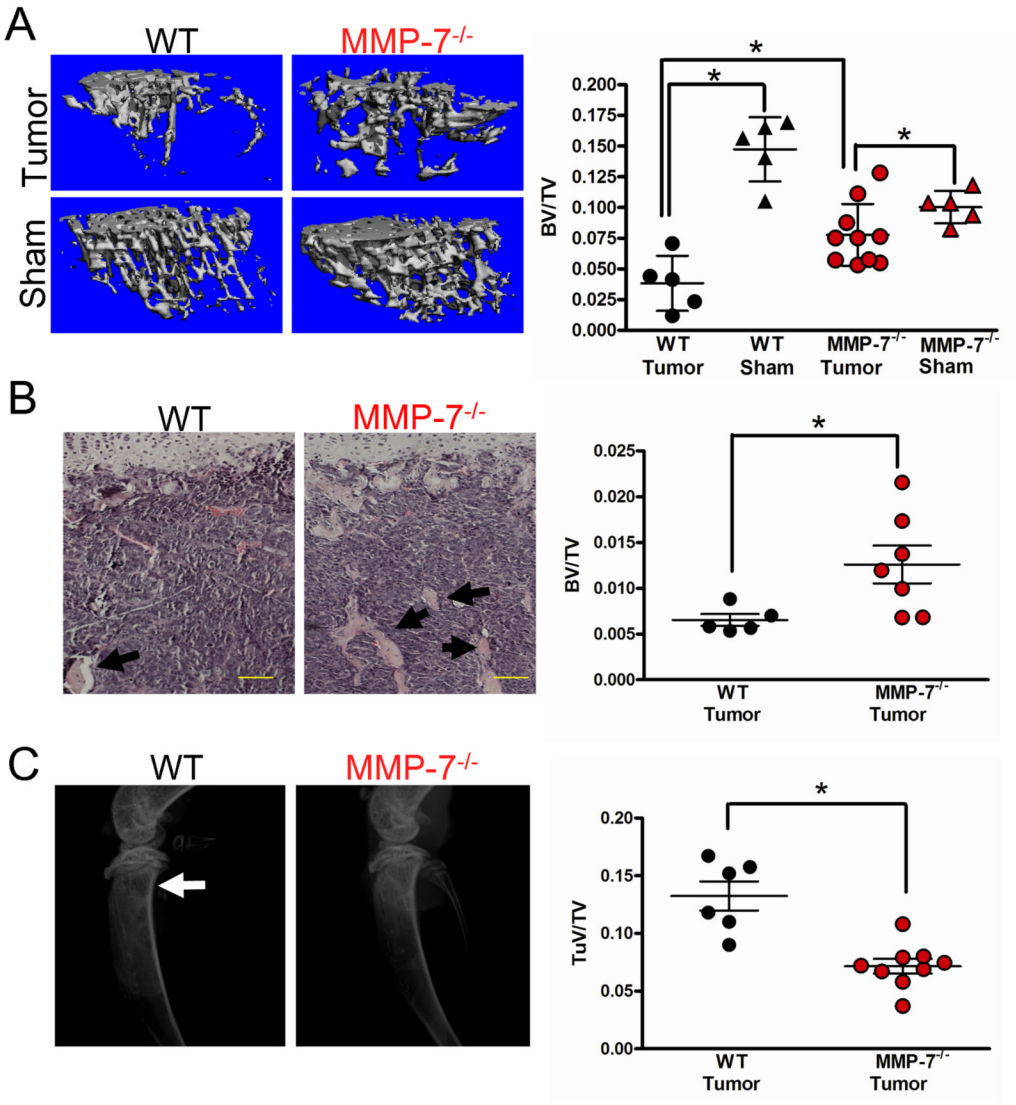

Figure 4.

Tumor mediated osteolysis is attenuated in the absence of host derived MMP-7. **A**: μCT scans of trabecular bone from tumor bearing and sham injected limbs of WT and MMP-7$^{-/-}$ animals allowed for the calculation of the BV/TV ratio. **B**: Representative H&E stained photomicrographs of tumor bearing tibias from WT and MMP-7$^{-/-}$ animals. Arrows indicate trabecular bone. Scale bars are 100μm. The BV/TV ratio was determined in several non-serial sections of tumor injected tibias obtained from WT (n=5) and MMP-7 null animals (n=7). **C**: Representative radiographic images from tumor injected WT and MMP-7$^{-/-}$ animals at day 9. Arrow indicates lytic tumor lesions in the wild type animals. The tumor volume (TuV) over tissue volume (TV) for tumor injected limbs of WT and MMP-7$^{-/-}$ animals was assessed. Data are mean ± SD. Asterisk denotes that $p<0.05$ while n.s. indicates a non-significant p value.

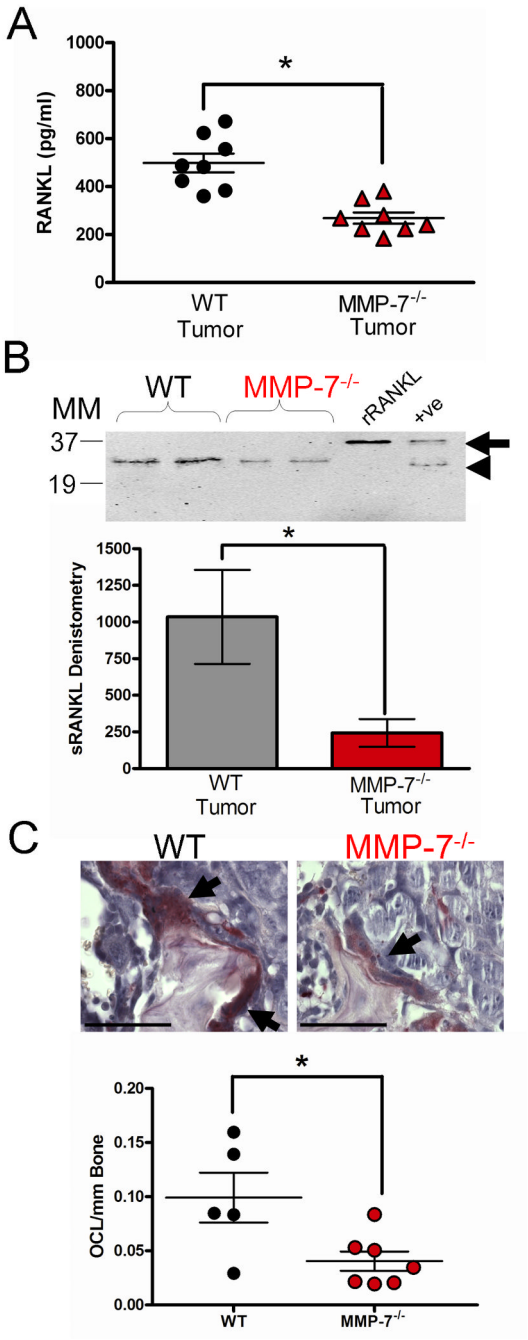

Figure 5.

MMP-7 solubilization of RANKL in the tumor-bone microenvironment. **A**: ELISA analysis of soluble RANKL levels in lysates from tumor injected tibias obtained from WT (n=8) or MMP-7$^{-/-}$ (n=8) animals. **B**: Representative immunoprecipitation blot using antibodies directed toward the N-terminus of RANKL for the detection of soluble RANKL in tumor bearing tibias of WT and MMP-7$^{-/-}$ animals. MM refers to the molecular weight marker in kDa. Unglycosylated full length recombinant RANKL (arrow) was used as a positive control. In addition, MMP-7 solubilized RANKL (arrow head) served as a further positive control (+ve). Densitometry was performed on the level of soluble RANKL in PyMT-Luc bearing limbs derived from wild type (n=11) and MMP-7$^{-/-}$ null (n=12) mice. **C**: TRAcP (red) positive,

multinucleated (blue) osteoclasts (arrows) at the tumor-bone interface in WT and MMP-7$^{-/-}$ animals. The number of osteoclasts at the tumor-bone interface were determined in multiple non-serial sections of tumor injected tibias obtained from WT (n=5) and MMP-7$^{-/-}$ (n=7) animals. Scale bars represent 100μm. Data are mean ± SD. Asterisk denotes that $p<0.05$ while n.s. indicates a non-significant p value.

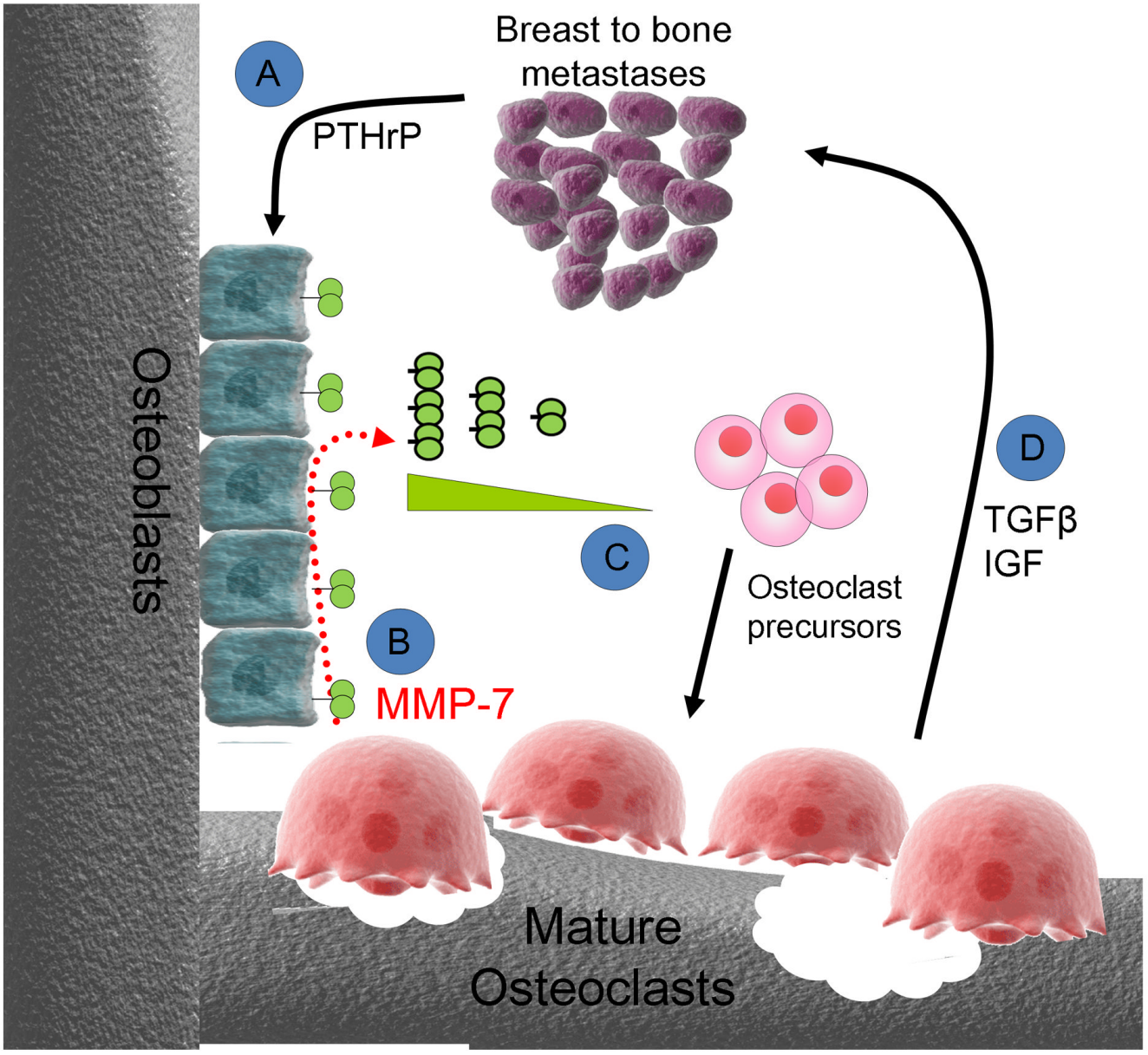

Figure 6.

Hypothetical mechanism of osteoclast derived MMP-7 action in the mammary tumor-bone microenvironment. **A**: Metastatic tumor cells through the secretion of factors such as parathyroid hormone related peptide (PTHrP), stimulate osteoblasts to express full length membrane bound RANKL. **B**: Osteoclasts express MMP-7 which can process membrane bound RANKL to a soluble active form. **C**: Soluble RANKL has been shown to be chemotactic for osteoclast precursors (25). In addition to acting as a potential chemotactic molecule, soluble RANKL can stimulate the maturation and activation of osteoclast precursors. **D**: Activated osteoclasts in turn execute bone resorption leading to the release of growth factors such as TGFβ and IGFs that promote tumor survival and growth in the bone microenvironment.